

# Crystal Structure of $\text{Eu}_2\text{PdSi}_3$

U. Ch. Rodewald<sup>a</sup>, R.-D. Hoffmann<sup>a</sup>, R. Pöttgen<sup>a</sup>, and E. V. Sampathkumaran<sup>b</sup>

<sup>a</sup> Institut für Anorganische und Analytische Chemie, Westfälische Wilhelms-Universität Münster, Wilhelm-Klemm-Straße 8, D-48149 Münster, Germany

<sup>b</sup> Department of Condensed Matter Physics & Materials Science, Tata Institute of Fundamental Research, Mumbai – 400 005, India

Reprint requests to R. Pöttgen. E-mail: pottgen@uni-muenster.de

Z. Naturforsch. **58b**, 971 – 974 (2003); received August 19, 2003

Single crystals of  $\text{Eu}_2\text{PdSi}_3$  were obtained from an arc-melted sample that was further annealed at 1020 K for seven days in a silica tube. The structure of  $\text{Eu}_2\text{PdSi}_3$  was refined from single crystal X-ray diffractometer data:  $P6/mmm$ ,  $a = 831.88(12)$ ,  $c = 435.88(9)$  pm,  $wR2 = 0.1175$ , 265  $F^2$  values, and 13 variable parameters. It crystallizes with the  $\text{U}_2\text{RuSi}_3$  structure, a superstructure of the  $\text{AlB}_2$  type. The palladium and silicon atoms form a planar two-dimensional  $[\text{PdSi}_3]$  network. The two crystallographically different europium atoms have hexagonal prismatic coordinations  $\text{Eu1Si}_{12}$  and  $\text{Eu2Pd}_4\text{Si}_8$ . The Pd–Si and Si–Si distances within the  $[\text{PdSi}_3]$  network are 244 and 236 pm, respectively.

**Key words:** Silicide, Crystal Structure, Solid State Synthesis

## Introduction

The  $\text{AlB}_2$  structure type allows a variety of different colorings on the boron network. Assuming a given  $\text{REX}_2$  ( $\text{RE}$  = rare earth element;  $X$  = element of the 3<sup>rd</sup>, 4<sup>th</sup> or 5<sup>th</sup> main group) compound, it is sometimes possible to substitute some of the  $X$  atoms by a  $T$  atom ( $T$  = transition metal) resulting in ternary intermetallic  $\text{RETX}$  or  $\text{RE}_2\text{TX}_3$  compounds. The structures of these compounds are ordered substitution variants of the aristotype  $\text{AlB}_2$  and their space groups derive from  $P6/mmm$  by symmetry reduction. In a recent review article [1] we discussed 46 structure types which belong to this family of compounds. The space group relations have been discussed according to the Bärnighausen formalism [2, 3].

In many cases, the symmetry reduction leads to two or more crystallographically independent rare earth sites, leading to interesting magnetic properties. This is also the case for the structure types  $\text{U}_2\text{RuSi}_3$  and  $\text{Ce}_2\text{CoSi}_3$  ( $P6/mmm$ ) [4–6],  $\text{Er}_2\text{RhSi}_3$  ( $P6_3/mmc$ ) [7, 8],  $\text{Ba}_4\text{Li}_2\text{Si}_6$  ( $Fddd$ ) [9], and  $\text{Ca}_4\text{Ag}_2\text{Si}_6$  ( $Fmmm$ ) [10] which all have two uranium (Er, Ba, Ca) sites. Although the four structures have the same composition, they exhibit a different puckering and packing of the  $[\text{TX}_3]$  networks. So far it is not possible to predict which of the four structure types a given  $\text{RE}_2\text{TX}_3$  compound adopts. The superstructure reflections resulting

from the *klassengleiche* symmetry reductions are all very weak and can easily be overlooked in an X-ray powder pattern. Only precise single crystal X-ray data can help to unambiguously determine the correct superstructure.

Also the silicide  $\text{Eu}_2\text{PdSi}_3$  [11–13] belongs to this family of  $\text{AlB}_2$  superstructures. So far  $\text{Eu}_2\text{PdSi}_3$  has only been characterized on the basis of X-ray powder data. Herein we report on the structure refinement based on single crystal diffractometer data.

## Experimental Section

### Synthesis

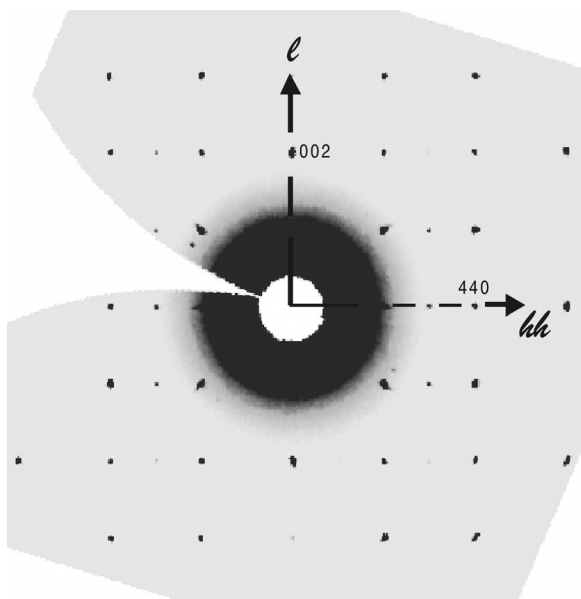
Starting materials for the preparation of  $\text{Eu}_2\text{PdSi}_3$  were europium ingots, palladium powder, and silicon pieces. A polycrystalline  $\text{Eu}_2\text{PdSi}_3$  sample was obtained by arc-melting of the elements under purified argon as described previously [14]. An excess of 5% europium was used to compensate the loss during the arc-melting process. The arc-molten button was subsequently sealed in an evacuated silica ampoule and annealed at 1020 K for 7 d. Compact pieces of  $\text{Eu}_2\text{PdSi}_3$  are light gray with metallic luster. The sample is stable in moist air. No decomposition was observed after several months.

### X-ray film data and structure refinement

Irregularly shaped single crystals were isolated from the annealed sample by mechanical fragmentation. They were

Table 1. Crystal data and structure refinement for  $\text{Eu}_2\text{PdSi}_3$ .

Empirical formula	$\text{Eu}_2\text{PdSi}_3$
Molar mass	494.59 g/mol
Unit cell dimensions (IPDS data)	$a = 831.88(12)$ pm $c = 435.88(9)$ pm $V = 0.2612$ nm <sup>3</sup>
Space group	$P6/mmm$ (No. 191)
Calculated density	6.29 g/cm <sup>3</sup>
Crystal size	$30 \times 40 \times 45$ $\mu\text{m}^3$
Transm. ratio (max/min)	1.27
Absorption coefficient	27.6 mm <sup>-1</sup>
$\theta$ Range	4° to 35°
Range in $hkl$	$-11 \leq h \leq 13$ , $-13 \leq k \leq 12$ , $-6 \leq l \leq 7$
Total no. reflections	3834
Independent reflections	265 ( $R_{\text{int}} = 0.0895$ )
Reflections with $I > 2\sigma(I)$	246 ( $R_{\text{sigma}} = 0.0389$ )
Data/parameters	265 / 13
Goodness-of-fit on $F^2$	0.882
Final $R$ indices [ $I > 2\sigma(I)$ ]	$R1 = 0.0316$ $wR2 = 0.1127$
$R$ Indices (all data)	$R1 = 0.0354$ $wR2 = 0.1175$
Extinction coefficient	0.0004(11)
Largest diff. peak and hole	2.29 and $-1.93$ e/Å <sup>3</sup>

Fig. 1. Reconstructed reciprocal  $hhl$  layer of  $\text{Eu}_2\text{PdSi}_3$ . Superstructure reflections are those with  $h = 2n + 1$ .

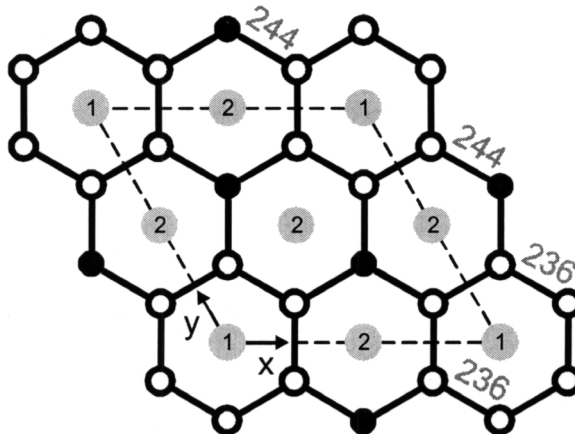
first examined on a Buerger precession camera in order to establish both symmetry and suitability for intensity data collection. Single crystal intensity data were collected at room temperature by use of a Stoe IPDS-II diffractometer with graphite monochromatized Mo- $K_\alpha$  radiation (71.073 pm) at a detector distance of 60 mm, an exposure time of 30 min,

Table 2. Atomic coordinates and anisotropic displacement parameters (pm<sup>2</sup>) for  $\text{Eu}_2\text{PdSi}_3$ .  $U_{\text{eq}}$  is defined as one third of the trace of the orthogonalized  $U_{ij}$  tensor.  $U_{13} = U_{23} = 0$ .

Atom	Wyckoff position	$x$	$y$	$z$	$U_{11}$	$U_{22}$	$U_{33}$	$U_{12}$	$U_{\text{eq}}$
Eu1	1a	0	0	0	80(4)	$U_{11}$	92(5)	40(2)	84(3)
Eu2	3f	1/2	0	0	89(4)	106(4)	109(5)	53(2)	100(3)
Pd	2d	1/3	2/3	1/2	68(4)	$U_{11}$	120(5)	34(2)	85(3)
Si	6m	0.1638(2)	2x	1/2	86(11)	73(12)	183(18)	37(6)	116(7)

Table 3. Interatomic distances (pm), calculated with the single crystal lattice parameters of  $\text{Eu}_2\text{PdSi}_3$ . All distances within the first coordination sphere are listed (standard deviations in parentheses).

Eu1:	12	Si	321.2(2)	Pd:	3	Si	244.3(3)
	6	Eu2	415.94(6)		6	Eu2	324.30(4)
	2	Eu1	435.88(9)	Si:	2	Si	236.0(3)
Eu2:	4	Pd	324.30(4)		1	Pd	244.3(3)
	8	Si	325.9(1)		2	Eu1	321.2(2)
	4	Eu2	415.94(6)		4	Eu2	325.9(1)
	2	Eu1	415.94(6)				
	2	Eu2	435.88(9)				

Fig. 2. Projection of the  $\text{Eu}_2\text{PdSi}_3$  structure onto the  $ab$  plane. Large gray, black filled, and medium open circles represent europium, palladium, and silicon, respectively. The two-dimensional  $[\text{PdSi}_3]$  network at  $z = 1/2$  is emphasized. Some relevant interatomic distances are indicated in units of pm.

and an omega range from 0 to 180° ( $\Delta\omega = 1^\circ$ ). The integration parameters were  $A = 14.5$ ,  $B = 5.0$ , and  $\text{EMS} = 0.02$ . A numerical absorption correction was applied to the data. All relevant details concerning the data collection are listed in Table 1.

Careful analyses of the data set showed a pronounced  $\text{AlB}_2$  type subcell and weak reflections doubling the  $a$  and  $b$  axes. The reciprocal layers  $hk0$  and  $hk1$  showed high Laue

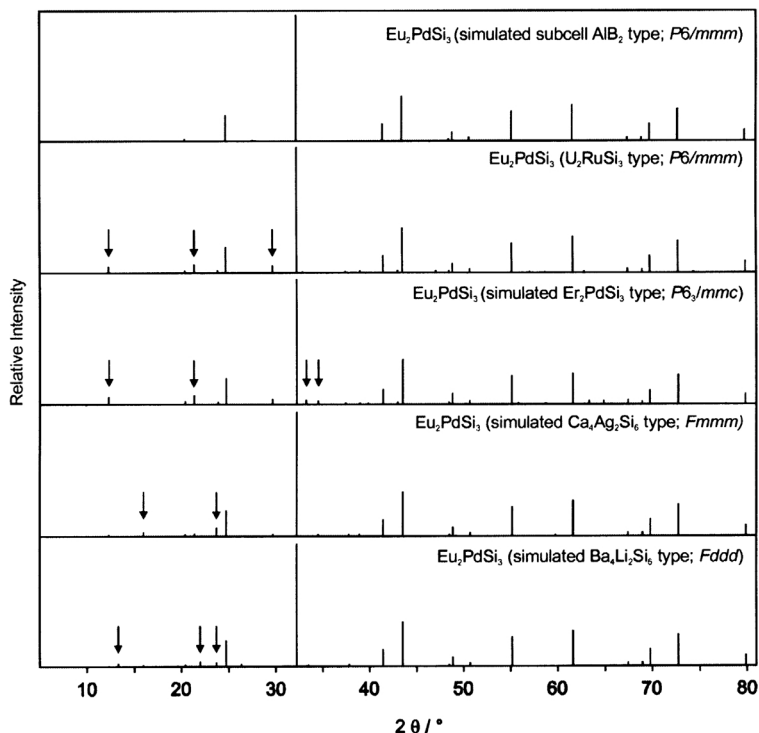


Fig. 3. Calculated powder patterns ( $\text{Cu-K}\alpha_1$  radiation) for the  $\text{AlB}_2$  type subcell and the  $\text{U}_2\text{RuSi}_3$  type superstructure of  $\text{Eu}_2\text{PdSi}_3$ . The other three diagrams are simulations for a possible  $\text{Er}_2\text{RhSi}_3$ ,  $\text{Ba}_4\text{Li}_2\text{Si}_6$ , or  $\text{Ca}_4\text{Ag}_2\text{Si}_6$  type superstructure for  $\text{Eu}_2\text{PdSi}_3$ . The unequivocal superstructure reflections for each superstructure model are marked by arrows. The observed powder pattern of ref. [11] is best matched by the calculation with the  $\text{U}_2\text{RuSi}_3$  type.

symmetry and no systematic extinctions, compatible with space groups  $P6/mmm$ ,  $P6mm$ ,  $P\bar{6}2m$ , and  $P\bar{6}m2$ . The space group with the highest symmetry,  $P6/mmm$  was found to be correct during the structure refinements. As mentioned in the introduction, four different structure types are known for the composition  $\text{RE}_2\text{TX}_3$ . We have therefore carefully analysed the reciprocal space. As is evident from the reconstructed  $hhl$  layer in Fig. 1, no doubling is observed for the  $c$  lattice parameter. Also no diffuse scattering is observed in this direction as well as in other directions, which would be relevant to a doubling of the  $c$  axis.

The atomic positions of  $\text{Ce}_2\text{CoSi}_3$  [6] were taken as starting values and the structure was successfully refined using SHELXL-97 (full-matrix least-squares on  $F_o^2$ ) [15] with anisotropic atomic displacement parameters for all sites. As a check for the correct composition, the occupancy parameters were refined in a separate series of least-squares cycles. All sites were fully occupied within two standard deviations. A final difference Fourier synthesis revealed no significant residual peaks (see Table 1). The positional parameters and interatomic distances are listed in Tables 2 and 3. Listings of the observed and calculated structure factors are available.\*

\*Details may be obtained from: Fachinformationszentrum Karlsruhe, D-76344 Eggenstein-Leopoldshafen (Germany), E-mail: crysdata@fiz-karlsruhe.de by quoting the Registry No. CSD-391246.

Although the refinement converged to quite low residuals for all reflections, we prefer to calculate separate residuals for the superstructure reflections [16], since the overall residual is strongly affected by the dominating subcell reflections. For a  $1\sigma$  cutoff we got a residual of 0.0742 for 182 superstructure reflections accounting for 27% of the total scattered intensity. The 83 subcell reflections yield a  $R1$  of 0.0174.

## Discussion

A projection of the  $\text{Eu}_2\text{PdSi}_3$  structure is shown in Fig. 2. The palladium and silicon atoms build a two-dimensional  $[\text{PdSi}_3]$  network. Within these networks the silicon atoms build discrete  $\text{Si}_6$  rings and the palladium atoms have a trigonal-planar silicon coordination at Pd–Si distances of 244 pm, close to the sum of the covalent radii of 246 pm [17]. The structure contains two crystallographically independent europium sites which both have a hexagonal prismatic coordination, Eu1 by 12 silicon atoms and Eu2 by four palladium and eight silicon atoms.

Such a two-dimensional network also occurs in  $\text{Ca}_4\text{Ag}_2\text{Si}_6$  [10]. Electron counting in the calcium compound may be written as  $(4\text{Ca}^{2+})^{8+}(2\text{Ag}^+)^{2+}[\text{Si}_6]^{10-}$ . According to magnetic suscepti-

bility measurements [11], the europium atoms in  $\text{Eu}_2\text{PdSi}_3$  are divalent, leading to a formulation  $(4\text{Eu}^{2+})^{8+}(\text{2Pd}^+)^{2+}[\text{Si}_6]^{10-}$  with a formal charge of +1 per palladium atom. The Si–Si distance within the  $10\pi$ -electron Hückel arenes  $[\text{Si}_6]^{10-}$  is 236 pm, similar to those in  $\text{Ba}_4\text{Li}_2\text{Si}_6$  [9] and  $\text{Ca}_4\text{Ag}_2\text{Si}_6$  [10], and elemental silicon [18]. The ionic formula splitting is certainly only a first rough approximation. Besides the strong Si–Si bonding we have to consider also the strong covalent Pd–Si bonds within the network.

The  $\text{U}_{33}$  displacement parameters of the palladium and silicon atoms are about two times larger than the  $\text{U}_{11}$  values. This might indicate a tendency for puckering of the  $[\text{PdSi}_3]$  network as it is realized in the  $\text{Er}_2\text{RhSi}_3$  structure [7, 8]. The X-ray powder (see below) and single crystal data, however, give no indication for an enlargement of the unit cell along the *c* direction. A similar behavior was recently observed for the  $[\text{CoSi}_3]$  network in  $\text{Ce}_2\text{CoSi}_3$  [6]. The displacements of the silicon atoms are much more pronounced

in  $\text{U}_2\text{RuSi}_3$  [4]. Here, the structure was even refined with a split position  $x\ 2x\ z$  instead of  $x\ 2x\ 1/2$ . However, the X-ray powder and single crystal data and electron diffraction patterns gave also no hint for a unit cell enlargement.

Finally we present calculated X-ray powder patterns ( $\text{Cu-K}\alpha_1$  radiation) [19] for the  $\text{AlB}_2$  type subcell and the  $\text{U}_2\text{RuSi}_3$  type superstructure of  $\text{Eu}_2\text{PdSi}_3$  in Fig. 3. The other three diagrams in that Figure are simulations for a possible  $\text{Er}_2\text{RhSi}_3$ ,  $\text{Ba}_4\text{Li}_2\text{Si}_6$ , or  $\text{Ca}_4\text{Ag}_2\text{Si}_6$  type superstructure for  $\text{Eu}_2\text{PdSi}_3$ . From the calculated patterns it can be seen that the different superstructures can clearly be distinguished from high quality X-ray powder data. The superstructure model derived here from the single crystal data is in excellent agreement with the powder pattern reported in ref. [11].

#### Acknowledgements

This work was financially supported by the Fonds der Chemischen Industrie and by the Deutsche Forschungsgemeinschaft.

- 
- [1] R.-D. Hoffmann, R. Pöttgen, *Z. Kristallogr.* **216**, 127 (2001).
  - [2] H. Bärnighausen, *Commun. Math. Chem.* **9**, 139 (1980).
  - [3] H. Bärnighausen, U. Müller, *Symmetriebeziehungen zwischen den Raumgruppen als Hilfsmittel zur straffen Darstellung von Strukturzusammenhängen in der Kristallchemie*. Universität Karlsruhe und Universität-GH Kassel, Germany, 1996.
  - [4] R. Pöttgen, P. Gravereau, B. Darriet, B. Chevalier, E. Hickey, J. Etourneau, *J. Mater. Chem.* **4**, 462 (1994).
  - [5] B. Chevalier, R. Pöttgen, B. Darriet, P. Gravereau, J. Etourneau, *J. Alloys Compd.* **233**, 150 (1996).
  - [6] R. A. Gordon, C. J. Warren, M. G. Alexander, F. J. DiSalvo, R. Pöttgen, *J. Alloys Compd.* **248**, 24 (1997).
  - [7] B. Chevalier, P. Lejay, J. Etourneau, P. Hagenmüller, *Solid State Commun.* **49**, 753 (1984).
  - [8] R. E. Gladyshevskii, K. Cenizal, E. Parthé, *J. Alloys Compd.* **189**, 221 (1992).
  - [9] H. G. von Schnering, U. Bolle, J. Curda, K. Peters, W. Carrillo-Cabrera, M. Somer, M. Schultheiss, U. Wedig, *Angew. Chem.* **108**, 1062 (1996).
  - [10] R. Cardoso Gil, W. Carrillo-Cabrera, M. Schultheiss, K. Peters, H. G. von Schnering, *Z. Anorg. Chem.* **625**, 285 (1999).
  - [11] R. Mallik, E. V. Sampathkumaran, M. Strecker, G. Wortmann, P. L. Paulose, *J. Magn. Magn. Mater.* **185**, L135, (1998).
  - [12] S. Majumdar, R. Mallik, P. L. Paulose, E. V. Sampathkumaran, *Physica B* **259–261**, 166 (1999).
  - [13] S. Majumdar, R. Mallik, E. V. Sampathkumaran, P. L. Paulose, K. V. Gopalakrishnan, *Phys. Rev. B* **59**, 4244 (1999).
  - [14] R. Pöttgen, Th. Gulden, A. Simon, *GIT Labor Fachzeitschrift* **43**, 133, (1999).
  - [15] G. M. Sheldrick, *SHELXL-97*, Program for Crystal Structure Refinement, University of Göttingen, Germany (1997).
  - [16] R.-D. Hoffmann, *RWERT*, Program for the Calculation of Separate Residuals for Superstructure Reflections, University of Münster (1996).
  - [17] J. Emsley, *The Elements*, Oxford University Press, Oxford (1999).
  - [18] J. Donohue, *The Structures of the Elements*, Wiley, New York (1974).
  - [19] K. Yvon, W. Jeitschko, E. Parthé, *J. Appl. Crystallogr.* **10**, 73 (1977).